Journal of Molecular Catalysis A: Chemical 316 (2010) 1–7

Contents lists available at ScienceDirect

Journal of Molecular Catalysis A: Chemical

journal homepage: www.elsevier.com/locate/molcata

Editor choice paper

The reactivity of surface active carbonaceous species with CO_2 and its role on hydrocarbon conversion reactions

Jianjun Guo[a,b], Hui Lou[a,*], Liuye Mo[a], Xiaoming Zheng[a,*]

[a] Institute of Catalysis, Department of Chemistry, Zhejiang University, Hangzhou 310028, PR China
[b] Ningbo Institute of Material Technology and Engineering, Chinese Academy of Science, Ningbo 315201, PR China

ARTICLE INFO

Article history:
Received 28 August 2009
Received in revised form
30 September 2009
Accepted 30 September 2009
Available online 8 October 2009

Keywords:
Coke
Ni catalyst
Carbon dioxide
Methane reforming
FTIR

ABSTRACT

Carbon deposition on Ni-based catalysts has a significant influence on their cracking activity and selectivity and is the main reason for catalyst deactivation. To understand this behavior, pulse techniques and in situ infrared spectroscopic analysis were applied to the study of the surface carbonaceous species formation and transformation over $Ni/MgAl_2O_4$, $Ni/MgO/\gamma\text{-}Al_2O_3$ and $Ni/\gamma\text{-}Al_2O_3$. It was found that $MgAl_2O_4$ allows an effective way for CO_2 adsorption and activation through the formation of formate/carbonate type species. Carbon adspecies, mainly as CH_x ($x = 1–3$), are the intermediates of methane activation on Ni particles and preferably diffuse from the metal to the interference of Ni and the supports and promote the adsorbed CO_2 species to decompose and release CO through formate/carbonate type intermediates. The mechanism proposed emphasis the role of these surface species in the surface chemistry of carbonaceous reaction. The data obtained led to a satisfactory description of the working catalyst.

1. Introduction

The formation of coke deposits leading to catalyst deactivation has been a challenge for catalytic technology in many hydrocarbon processes. The indirect and direct conversion of nature gas both on oxidative and non-oxidative conditions are examples of such developments [1]. In these cases, the effective management of catalyst deactivation and catalyst regeneration is the key in many heterogeneously catalyzed processes. The optimization of such complex processes requires the characterization of the coke formation process and its reactivity in order to understand the effect of the operational variables on these deposits and, therefore, minimize its accumulation and develop effective regeneration strategies.

Several characterization techniques [2], such as temperature-programmed oxidation, X-ray photoelectron spectroscopy (XPS), high-resolution electron microscopy, and Raman spectroscopy, have been used to study coke deposits and to obtain information regarding the deactivation mechanism and regeneration conditions. Previously, we used temperature-programmed reaction techniques and Raman spectroscopy to characterize coke species deposited on a $5\%Ni/MgAl_2O_4$ catalyst [3], which exhibits high activity and significant stability during dry reforming of methane [4,5]. It was found that two main properties of a catalyst affect the carbon deposition: surface structure and surface acidity. The nature and quantity of the coke is strongly dependant on the composition of the reacting feed, reaction time and temperature. There are three carbon species (i.e., C_α, C_β and C_γ) on the catalyst surface, in which C_γ was graphite-like carbon species and was responsible for catalyst deactivation. The nature of the carbon species can also be classified as polymeric, filamentous, and graphitic [6]. Polymeric coke is supposed to be derived from thermal decomposition of hydrocarbons, whereas the filamentous and graphitic forms of coke are formed on the catalyst. Coke can also be characterized based on its reactivity with hydrogen, water and oxygen. Although these are gross properties that do not provide detailed chemical information, they are closely related to the actual reaction conditions. Although coke characterization has been included in many papers, there are still some disputations about the accurate mechanism details. Different surface species on Ni catalysts were also identified on different supports. In situ diffuse reflectance fourier transform infrared spectroscopy (DRIFTS) revealed that CH_x can react with OH species from the support, and CH_xO species were formed on TiO_2 and Al_2O_3-supported transition metals [1,7]. While on La_2O_3 supported transition metals, oxycarbonates were found to be the main intermediate [8,9]. Further, it is argued that the CO_2 was activated on support or Ni particles are also involved.

In the present study, the bulk structure of surface carbonaceous species and its reactivity with various gases were further investigated using X-ray diffraction (XRD), pulse experiments and in situ

* Corresponding authors. Tel.: +86 571 88273593; fax: +86 571 88273283.
E-mail addresses: hx215@zju.edu.cn (H. Lou), xmzheng@dial.zju.edu.cn (X. Zheng).

1381-1169/$ – see front matter © 2009 Elsevier B.V. All rights reserved.
doi:10.1016/j.molcata.2009.09.023

DRIFTS. Emphasizes was placed on the surface species formation and transformation on the catalysts during dry reforming reactions. The satisfactory description of the coking activity and a possible role in hydrocarbon conversion reactions was proposed in the light of the results obtained.

2. Experimental

2.1. Catalyst characterization

Magnesium aluminate spinel ($MgAl_2O_4$) was prepared in a similar way to previous studies [4]. Stoichiometric quantities of $Mg(NO_3)_2{\cdot}6H_2O$ and $Al(NO_3)_3{\cdot}9H_2O$ were dissolved separately in distilled water. The resulting solutions and an aqueous solution of ammonia were dropped into a flask at the same time with constant stirring to maintain the pH value at about 9.5. The precipitate was continuously stirred for an hour and then aged overnight. After being thoroughly washed with distilled water for several times, the resulting slurry was then dried at 120 °C for 15 h and calcined at 800 °C for 8 h in air.

Supported nickel catalyst was prepared by conventional wet impregnation, using nitrate salt as the precursor. A given amount of nickel nitrate solution was placed in a 100 ml beaker, the appropriate amount of $MgAl_2O_4$ or γ-Al_2O_3 was added under continuous stirring. The slurry was dried at 120 °C over night and calcined at 550 °C under air for 5 h.

2.2. Catalytic testing

The CO_2 reforming of methane was carried out at 750 °C and atmospheric pressure, using 20 mg catalyst (unless otherwise mentioned) in a fixed-bed quartz reactor (ca. 4 mm i.d.). Activation of the Ni-catalyst involved reductive treatment with hydrogen at 750 °C for 60 min. The reactant feed was CH_4:CO_2 = 1:1 and a flow rate of 30 ml/min. The exit gases were analyzed with an on-line gas chromatograph equipped with a TCD, using a TDX-01 column. The conversions and selectivity were calculated on the basis of the reforming reaction and the water–gas shift reaction [10].

Pulse reactions were performed in a conventional flow system with a flow measuring and control system, a mixing chamber, and a fixed-bed quartz reactor (4 mm i.d., 200 mm length), which was placed in an electric oven. Before reaction, the catalysts were reduced in situ at 750 °C for 60 min in H_2 flow. Before the pulse data were obtained, the catalyst was treated in situ at 750 °C for 30 min in flowing Ar. The reactant was introduced with a 6-port gas sampling valve under a stream of Ar carrier gas. Analysis of the gases during the pulsed reactions was done by an on-line quadrupole mass spectrometer (OmniStar GSD 301), which scanned peaks of the following eight compounds: H_2, CH_4, $^{13}CH_4$, H_2O, CO, ^{13}CO, CO_2, $^{13}CO_2$ within 1 s.

2.3. Catalyst characterization

The crystal structure of catalysts before and after reaction was determined by XRD in a Rigaku D/max-IIIB apparatus using Cu $K_{\alpha 1}$ radiation (λ = 1.54056 Å), at 45 kV and 40 mA. Diffraction peaks recorded in a 2θ range between 20° and 70° have been used to identify the structure of the samples. The apparent crystallite size was determined using the Scherrer formula with standard procedure [11].

Nickel dispersion was determined by H_2 chemisorption at room temperature in a pulse experimental apparatus. The catalyst was reduced by H_2 at 750 °C for 2 h. Then the temperature was decreased to 100 °C under Ar, kept there for 20 min, and then further decreased to room temperature for the in situ H_2 chemisorption measurements. The quantity of H_2 adsorbed at monolayer coverage and the mean particle sizes of Ni were obtained by a standard procedure [12].

2.4. In situ DRIFTS

DRIFTS experiments were performed on a Nicolet 740 FTIR spectrometer equipped with an in situ DRIFTS cell with KBr windows. The cell was cooled by water circulating, which allowed collection of spectra over the temperature range between 25 °C and 700 °C at atmospheric pressure. The interaction of CO_2, CH_4 or the reaction mixture with both the support and the catalyst was studied. In all cases, the sample was reduced under a flowing H_2/He mixture for 2 h and purged with He for additional 0.5 h at 700 °C. Then a flow of CH_4/He, CO_2/He or the reaction mixture was introduced into the DRIFTS cell. The spectra of the adsorbed specie were obtained by subtraction of the initial spectrum registered after the reduction step. For all the spectra recorded, a 32-scan data accumulation was carried out at a resolution of 4 cm^{-1}.

3. Results

3.1. Catalyst characterization and catalytic performance

The XRD patterns of $MgAl_2O_4$ supported Ni catalysts were quite simple [4]. The diffraction lines of Ni/$MgAl_2O_4$ catalyst virtually coincided with those of the as-prepared $MgAl_2O_4$ support and no other lines of Ni-containing species were discerned. However, NiO diffraction lines were depicted with the Ni/γ-Al_2O_3 and Ni/MgO–Al_2O_3 catalysts. This implies that the NiO in the as-prepared Ni/$MgAl_2O_4$ catalysts was finely dispersed (with a dispersion of 16%, Table 1), which could be responsible for the higher

Table 1
Properties, catalytic behavior and coking of 5%Ni/γ-Al_2O_3 and 5%Ni/$MgAl_2O_4$ catalysts[a].

Catalyst	H_2 uptake ($cm^3\ g^{-1}$)	Ni dispersion (%)	Conversion (%)		Selectivity (%)		Metallic particle size of Ni^0 (nm)		Coke[b] (wt.%)
			CH_4	CO_2	H_2	CO	Before reaction	After Reaction	
Ni/γ-Al_2O_3	0.2896	3	59.1	61.0	82.9	94.2	26.5[c] 110[d] 19.6[f]	90.0[c] n.d.[e] n.d.	14.5
Ni/$MgAl_2O_4$	1.5797	16	82.6	87.7	97.5	93.8	10.4[c] 20[d] 8.8[f]	11.8[c] n.d. 10.1[f]	1.2

[a] Reaction conditions: T = 750 °C; catalyst, 50 mg; GHSV = 50,000 ml/(g-cat h); CH_4:CO_2 = 1.0:1.0; P = 1 atm.
[b] Coke deposition was quantified by thermogravimetry after 10 min on stream.
[c] Determined by XRD.
[d] Determined by H_2 chemisorptions assuming that each surface metal atom chemisorbs one hydrogen atom, i.e., $H/Ni_{surface}$ = 1.
[e] n.d., not determined.
[f] Determined by TEM.

stability and lower carbon deposition of the $Ni/MgAl_2O_4$ catalyst in dry reforming of methane. The mean nickel particle sizes estimated by employing Scherrer's equation following the standard procedures are of the order of 10.4 nm and 11.8 nm before and after 10 h on stream as indicated in Table 1. These are in accordance with values derived from transmission electron microscopy (TEM) results (Table 1), in which the Ni^0 particle size increased from 8.8 nm to 10.1 nm. This indicates that Ni particle sintering occurs under the reaction conditions. Sintering is an important route for the deactivation of Ni-based dry reforming catalysts. However, the particle size only increased about 15% in the first 10 h and this did not induce deactivation, as demonstrated in Table 1. This is because the catalyst can produce a highly dispersed active phase and a large active surface area as bound-state Ni species after pre-reduction. In contrast, the $Ni/\gamma\text{-}Al_2O_3$ catalyst has a relatively lower Ni dispersion and sintered severely during the reaction (the particle size increased about 300% as indicated in Table 1). This implies that a proper interaction exists between Ni and $MgAl_2O_4$, which contribute to the high dispersion of Ni and inhibit the sintering of Ni particles, as has been discussed [4].

We have studied the activity and stability of the as-prepared catalysts in differential condition. As shown in Table 1, $Ni/MgAl_2O_4$ gives superior high activity than Ni/Al_2O_3 toward dry reforming of methane. The ratio of H_2/CO obtained under the stated conditions was found to vary between 0.78 and 1.01 for Ni/Al_2O_3 and $Ni/MgAl_2O_4$, respectively. Long-term stability tests indicate that the activity of $Ni/MgAl_2O_4$ catalyst remained unchanged over 55 h on stream, while Ni/Al2O3 deactivated quickly in 10 h [4,5]. It has been established that the primary reason for deactivation of $Ni/\gamma\text{-}Al_2O_3$ can be generally attributed to carbon deposition on the Ni crystallites. As also shown in Table 1, the amount of coke reached about 14.5 wt% on $Ni/\gamma\text{-}Al_2O_3$, while only 1.2% was found on $Ni/MgAl_2O_4$ after 10 min on stream. With the time on stream, it was found that the coking rate decreased on both catalysts, but $Ni/\gamma\text{-}Al_2O_3$ deactivated quickly owing to the large amount of coke accumulation, which plugs the reactor in around 10 h [4,5].

3.2. Surface active carbonaceous species

Although most researchers agree that carbon formation is the primary reason for the catalyst deactivation, disagreement exists on the source of the carbon. In our previous study [3], the amount of coke species deposited from CO disproportionation was found to be too small compared to CH_4 decomposition and was negligible during dry reforming of methane on $Ni/MgAl_2O_4$, which suggested that the main source of coke during the reaction was originated from CH_4 decomposition. The nature of these carbon species was further studied by in situ Fourier transform infrared spectroscopy (DRIFT), which was shown in Fig. 1. When a large amount of methane was introduced, the intense gaseous CH_4 adsorption at 2900–3050 cm^{-1} appeared. While no CH_x species was observed under the reaction conditions even at 500 °C (not shown). As a result, it hardly detect CH_x (x = 1–3) species even though CH_x species was widely accepted as an intermediate species for methane activation during CO_2 reforming of methane. It should be noted that the concentration of a species on the surface depends on its formation and conversion rates. The importance of a surface species in a catalytic cycle cannot be simply determined by its surface concentration or coverage. Many research groups have evidenced the existence of CH_x species by CD_4/H_2 and CH_4/D_2 isotopic transient reactions [13] and pulsed surface reaction analysis [14]. Indeed, a detailed spectrum of the C–H bands can be obtained after flushing the reacting gas phase with argon after 10 min on stream. Although weak and poorly resolved, the main bands around 2966 cm^{-1}, 2906 cm^{-1}, and 2871 cm^{-1} can be assigned to asymmetric and symmetric stretching vibrations of $-CH_3$ and $=CH_2$ species. A weak shoulder at around 2890 cm^{-1} also suggests the presence of some ≡CH groups [15]. In situ oxidation of the reacted sample was carried out subsequently. The CH_x bands described above disappeared, restoring the reference spectrum after 5 min.

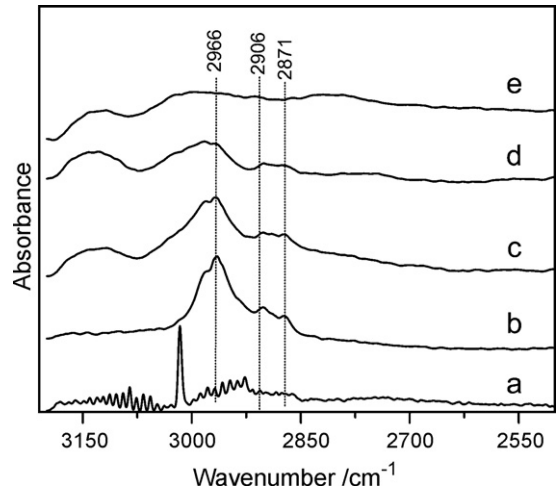

Fig. 1. Spectral detail of C–H absorption band region over $5\%Ni/MgAl_2O_4$ under different conditions: (a) under CH_4/CO_2 for 10 min; (b) after purge with N_2 for 20 min; (c) after TPO for 1 min; (d) after TPO for 2 min; (e) after TPO for 5 min at 650 °C.

3.3. Transient response reactions

Two sequences of pulsed reactions were conducted over $Ni/\gamma\text{-}Al_2O_3$ and $Ni/MgAl_2O_4$ catalysts. Fig. 2 shows responses to $^{13}CH_4$ pulse into 10% $^{12}CO_2$/Ar steady flow with $Ni/\gamma\text{-}Al_2O_3$ and $Ni/MgAl_2O_4$ at 750 °C. Signals of $^{12}CO_2$ were omitted from the profile. When $^{13}CH_4$ was introduced, H_2, ^{13}CO, ^{12}CO and $^{13}CO_2$ were generated immediately on $Ni/MgAl_2O_4$ and the signals of ^{12}CO and $^{13}CO_2$ reached a maximum at about 4 s later than those of ^{13}CO and H_2. This indicates that CO_2 and CH_4 were activated separately. The reaction process is likely preceded by rapid hydrogen abstraction from CH_4 to give adsorbed CH_x and H species, followed by a slow reaction of CO_2 with adsorbed CH_x species. The adsorbed H may assist CO_2 dissociation on both Ni and support surface since generation of ^{12}CO was also improved by $^{13}CH_4$ introduction, as reported by Osaka over various catalysts [16].

After $^{13}CH_4$ pulse passed through the catalyst bed, H_2, ^{13}CO, ^{12}CO and a very small amount of $^{13}CO_2$ were continued to evolve. Similar results were observed over $Ni/\gamma\text{-}Al_2O_3$ catalyst. While the conversion of CH_4 was much lower over $Ni/\gamma\text{-}Al_2O_3$ than that over $Ni/MgAl_2O_4$. This may be due to a lower dispersion of the active metal species on $Ni/\gamma\text{-}Al_2O_3$ catalyst [4].

Fig. 3 shows responses to pulsing CO_2 into 10% CH_4/Ar steady flow over $Ni/MgAl_2O_4$ and $Ni/\gamma\text{-}Al_2O_3$ catalyst. In this case, surface carbonaceous species (i.e., $-CH_3$, $=CH_2$ and ≡CH) were formed previously and continuous during the pulse reaction. When CO_2 was introduced, formation of CO was detected immediately over $Ni/MgAl_2O_4$, indicating of rapid CO_2 dissociation over Ni and $MgAl_2O_4$ perimeter. H_2 response started to reinforce after a few seconds. CO and H_2 continued to appear after CO_2 passed through the catalyst bed. When the same reaction was conducted on $Ni/\gamma\text{-}Al_2O_3$, only very small amount of CO_2 reacted and a small amount of H_2 and CO produced. This is due to the very weak adsorption of CO_2 on $\gamma\text{-}Al_2O_3$, unlike the case on $MgAl_2O_4$ support, where CO_2 is able to be concentrated after CO_2 pulses. Large amount of CH_x species were formed on both catalysts under CH_4 steady flow. But due to the weaker activation of CO_2 on $Ni/\gamma\text{-}Al_2O_3$, the reaction of CO_2 with CH_x occurred more slowly and the response of CO was very weak as compared to that of $Ni/MgAl_2O_4$.

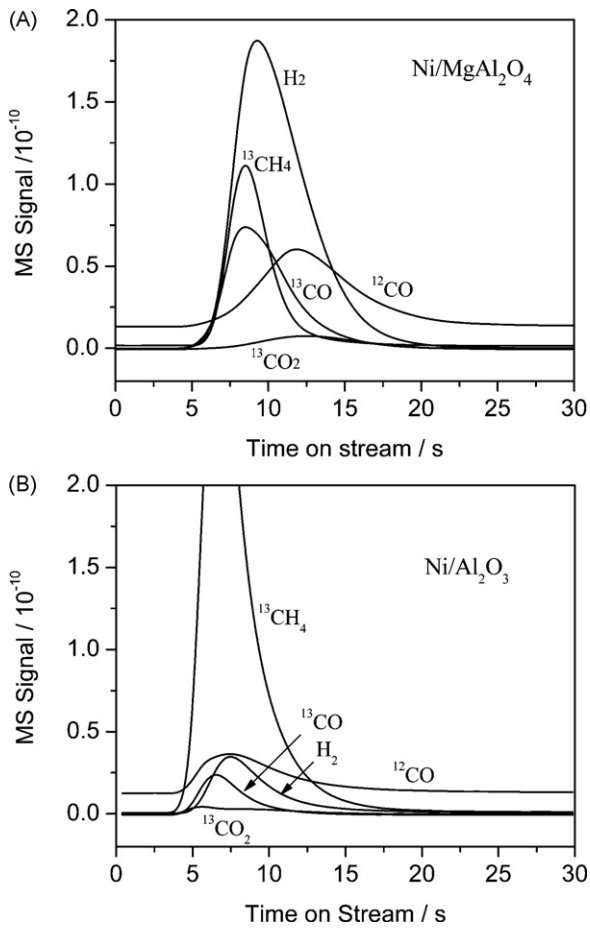

Fig. 2. Response to $^{13}CH_4$ pulse into 10%CO_2/Ar steady flow over 5%Ni/$MgAl_2O_4$ and 5%Ni/Al_2O_3 at 750 °C.

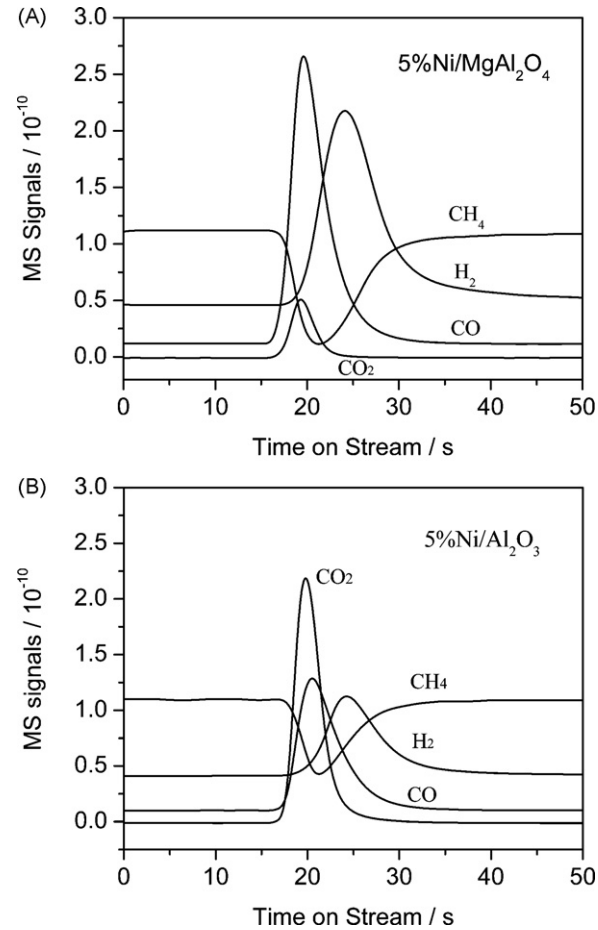

Fig. 3. Response to CO_2 pulse into 10%CH_4/Ar over 5%Ni/$MgAl_2O_4$ and 5%Ni/Al_2O_3 at 750 °C.

3.4. DRIFTS

DRIFTS experiments were conducted in CH_4, CO_2 or CH_4/CO_2 gas flows at 680 °C with the objective of identifying the adsorbed carbonaceous species under reaction conditions. Experiments were also conducted where changes in the IR spectrum were monitored in response to changes in the gas phase mixture induced by substituting the reactant mixture by diluted methane or carbon dioxide.

3.4.1. Surface active species on catalyst supports

DRIFTS of the $MgAl_2O_4$ support and the Ni/$MgAl_2O_4$ catalyst after adsorption of CO_2 and CH_4/CO_2 mixture are shown in Figs. 4 and 5 separately. Apart from the gas phase contributions of CO_2 centered ca. 2349 cm^{-1}, $^{13}CO_2$ centered ca. 2275 cm^{-1} or CH_4 at 1305 cm^{-1} and 3015 cm^{-1}, several bands in the region between 1200 cm^{-1} and 1600 cm^{-1} became apparent. On the support (in Fig. 4), two well-defined bands centered at 1500 cm^{-1} and 1293 cm^{-1} are observed after introduction of CO_2. The IR intensities of these two bands increase with increasing temperature and time on stream. These bands could be attributed to the carbonate type species adsorbed on the support at high temperature [17]. In addition, two shoulder bands centered at 1580 cm^{-1} and 1400 cm^{-1} also appeared and followed the same trends as carbonate species. These two bands can be assigned to asymmetric C–O and H–C–O stretching of adsorbed HCO_2^- [18]. Isolated O–H stretching mode of alumina hydroxyl was apparent at 3609 cm^{-1}. Meanwhile, three well-defined bands centered at 3726 cm^{-1}, 3702 cm^{-1} and 3618 cm^{-1} were appeared after CO_2 introduction due to the Fermi resonance of linearly adsorbed CO_2 [19].

DRIFTS of the hydrogen-treated support after exposure to the reacting mixture at 680 °C are shown in Fig. 5. When methane was introduced into the reacting mixture, the intensity of the band around 1500 cm^{-1} was reduced. After methane introduction, bands at 2170 cm^{-1} and 2115 cm^{-1} were observed and can be assigned to gaseous CO. The intensity of gaseous CO decreased with time on stream and reached a constant value after 30 min. It can be seen in Fig. 5 that the intensity of gaseous CO and carbonate species did not

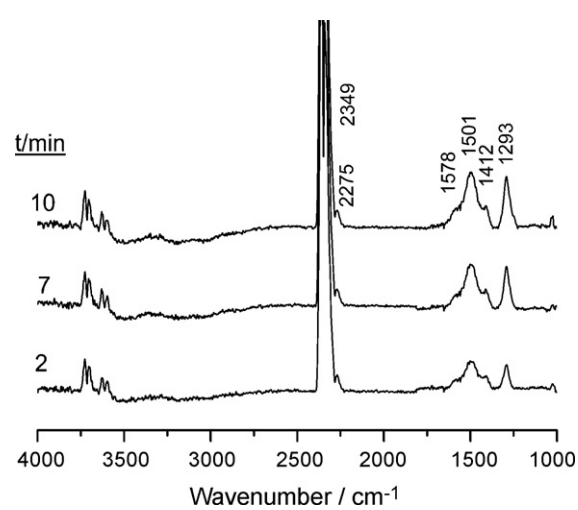

Fig. 4. DRIFT spectra of CO_2 adsorption at 680 °C on $MgAl_2O_4$. The reference spectrum was that of the sample prior to gas admission.

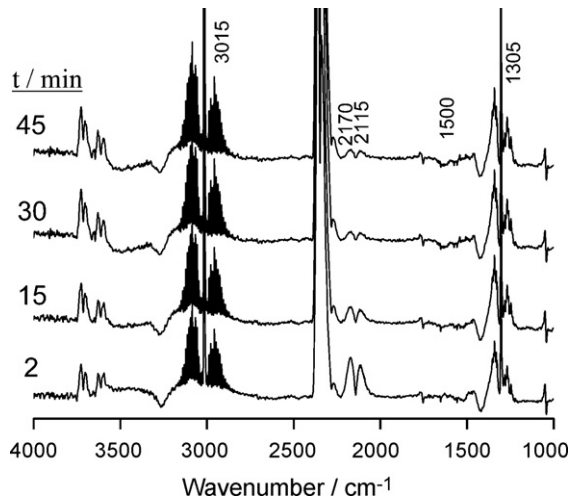

Fig. 5. DRIFT spectra of CH_4/CO_2 reforming on pretreated $MgAl_2O_4$ with CO_2 at 680 °C. The reference spectrum was that of the sample prior to gas admission.

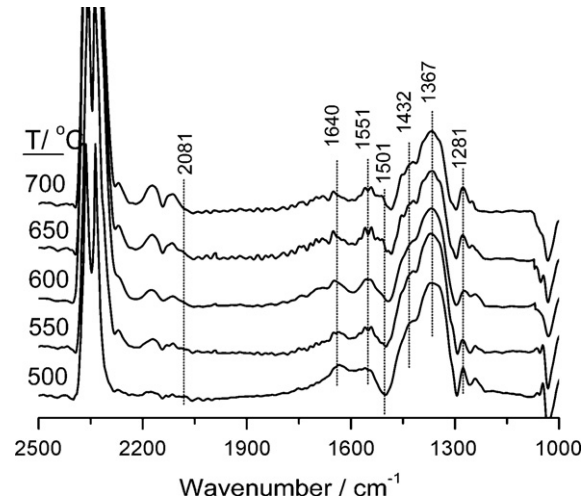

Fig. 7. DRIFT spectra of CH_4/CO_2 reforming on pre-reduced 5%Ni/$MgAl_2O_4$. The reference spectrum was that of the sample prior to gas mixture admission.

change as a function of time on stream after introduction of CH_4 for 30 min.

3.4.2. Surface active species on catalysts

In another experiments, Ni/$MgAl_2O_4$ was reduced in situ at 700 °C for 1 h in flowing hydrogen. After purging with Ar for 30 min, the gas flow was switched to 10%CO_2 + Ar or 10%CH_4 + 10%CO_2 + Ar. The surface species were also monitored by DRIFTS, and the results are shown in Figs. 6 and 7. Over Ni/$MgAl_2O_4$, similar tendencies were observed as on $MgAl_2O_4$ after introduction of CO_2 (Fig. 6). The adsorbed formate (bands at ca. 1410 cm^{-1} and 1551 cm^{-1}) and carbonate (bands at ca. 1501 cm^{-1} and 1291 cm^{-1}) species appeared after 2 min of CO_2 introduction and its intensity increased with time on stream.

In CH_4–CO_2 co-feeding conditions, large amount of formate ($\nu_{s,c=o}$ = 1367 cm^{-1}, $\nu_{as,c=o}$ = 1551 cm^{-1}) and carbonate ($\nu_{as,c=o}$ = 1640 cm^{-1}, $\nu_{s,c=o}$ = 1432 cm^{-1}, 1281 cm^{-1}, δ_{C-O} = 1230 cm^{-1}) species were formed. Efstathiou et al. [20] found that the formate species on Al_2O_3 surface was stable under CH_4/CO_2 reforming condition even at 500–600 °C. In the present study, the formate species formed were quite similar to those over Al_2O_3. The intensity of these bands indicated that the presence of CH_x, i.e., adsorbed H species, favors the formation of formate species first. With the increase of temperature to above 600 °C, the adsorption of formate species weakened, while the intensity of carbonate species (at 1510 cm^{-1} and 1281 cm^{-1}) increased accordingly. Over these catalysts, the formate species may transformed to carbonate species under a higher temperature.

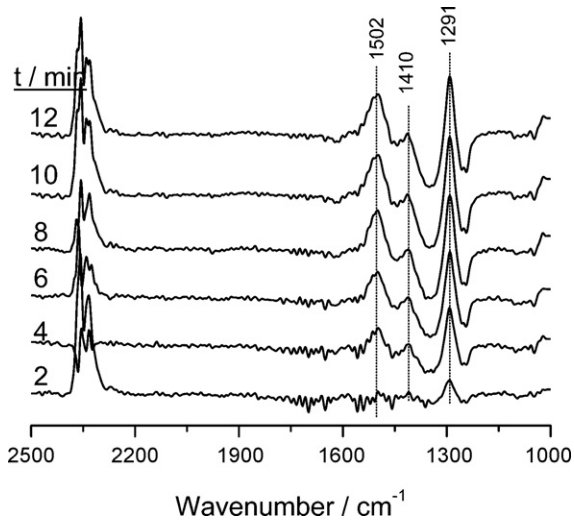

Fig. 6. Adsorption of CO_2 over 5%Ni/$MgAl_2O_4$ at 680 °C. The reference spectrum was that of the sample prior to CO_2 admission.

From the above experiments, no adsorbed CO and CH_x species were observed by in situ Fourier transform infrared spectroscopy (FTIR). Kroll et al. [21] observed intense band, due to linear and multi-bonded CO species, developed at 2012 cm^{-1} and 1855 cm^{-1}, respectively after introduction of the reaction mixture on Ni/SiO_2 catalyst at 500 °C. The lack of IR bands corresponding to adsorbed CO in the spectra of our samples suggests that the rate of desorption is greater than its formation at 680 °C.

4. Discussion

One of the major problems encountered in the activation of hydrocarbons over metal catalysts is the rapid accumulation of coke, which leads to blocking the active sites and deactivating the catalyst activity. However, in contrast to 5%Ni/Al_2O_3 catalyst which exhibit rapid deactivation during CO_2 reforming of methane, no deactivation was observed during 55 h on stream over a 5%Ni/$MgAl_2O_4$ catalyst [4]. In the 5%Ni/Al_2O_3 catalyst, Ni dispersion is very low. Based on the H_2 adsorption experiments, the Ni^0 average particle size of 5%Ni/Al_2O_3 catalyst is of the order of 110 nm, which are approximately 5 orders of magnitude higher than that of 5%Ni/$MgAl_2O_4$ catalyst. TEM showed that the Ni^0 average particle size of 5%Ni/$MgAl_2O_4$ was 8.8 nm, which was in agreement with the measurements from H_2 adsorption results and XRD results. In any event, the three techniques applied show that the Ni particle size is small on the $MgAl_2O_4$ support. After on stream for 10 h, the Ni particle size increased by only 13% over Ni/$MgAl_2O_4$, compared to approximately 300% of Ni/Al_2O_3. As have been reported [4], the particle size of $MgAl_2O_4$ was only 8.9 nm by XRD, which is comparable to 10.4 nm of the Ni particles. A nanocomposite catalyst may be formed between $MgAl_2O_4$ and size-comparable Ni-metal nanocrystals. The unusual interactions between these nanocomposite catalysts may contribute to the high dispersion of active metals and extremely stable catalysis [22].

The active oxygen species have important impact on the inhibition of inert carbonaceous species formation. An “oxygen pool” was proposed to be formed on the catalyst surface during CO_2 decomposition [23]. This causes the decreasing of CO_2 conversion

and formation of CO_2 instead of CO when reacted with surface CH_x species. Fig. 2 of present study $^{13}CO_2$ was observed over both Ni/Al_2O_3 and $Ni/MgAl_2O_4$ after pulsing $^{13}CH_4$ into 10%CO_2/Ar steady flow. Over $Ni/MgAl_2O_4$, $^{13}CO_2$ continued to evolve after $^{13}CH_4$ pulse passed through the catalyst bed, while this is not observed over Ni/Al_2O_3. These results indicate that the following reactions occurred over these catalysts:

$$^{13}CH_4(a)\text{–}Ni^0 \rightarrow {}^{13}CH_x\text{–}Ni^0 + H_2(g) \quad \text{rapid} \tag{1}$$

$$H\text{–}Ni^0 + {}^{12}CO_2\text{–}MgAl_2O_4 \rightarrow OH\text{–}MgAl_2O_4 + {}^{12}CO\text{–}Ni^0 \quad \text{rapid} \tag{2}$$

$$^{12}CO_2(a)\text{–}MgAl_2O_4 + {}^{13}CH_x\text{–}Ni^0 \rightarrow {}^{12}CO(g) + {}^{13}CO(g) + (x/2)H_2(g) + Ni^0\text{–}MgAl_2O_4 \quad \text{slow} \tag{3}$$

This implies that "oxygen pool" did form over these two catalysts in a large amount of CO_2, and this is so prominent over $Ni/MgAl_2O_4$ than over Ni/Al_2O_3. In the FTIR spectra, both $MgAl_2O_4$ and $Ni/MgAl_2O_4$ in the presence of CO_2 displayed several intense bands in the 1600–1300 cm^{-1} region, which can be assigned to carbonate/bicarbonate type species. These adsorption bands were depressed largely by the introduction of CH_4 subsequently. CH_x species formation was conformed also by FTIR experiments in Fig. 1. During the reaction, CO_2 may rapidly react with $MgAl_2O_4$ to generate carbonate/bicarbonate type species, which in turn reacts slowly with the CH_x species to generate the other main products, H_2 and CO. This slow reaction occurs most likely at the metal/support interface. As indicated in Fig. 5, there established a steady state between the surface carbonate species and the gaseous CO production when CH_4 was introduced to carbonate/bicarbonate type species covered catalyst. The presence of $MgAl_2O_4$ may promote the adsorption of CO_2 and formation of carbonate intermediate. The formation and reaction equilibrium of carbonate/bicarbonate type species sustained the high activity of $Ni/MgAl_2O_4$ catalyst.

On the other hand, $Ni/MgAl_2O_4$ and Ni/Al_2O_3 give similar response to CO_2 pulse into 10%CH_4/Ar. CO was detected immediately when CO_2 was introduced. Interestingly, H_2 was started to appear after a few seconds. This implies that CO_2 was firstly adsorbed on the support and dissociated into gaseous CO and adsorbed O species, which in turn reacted with surface CH_x to release CO:

$$CO_2\text{–}MgAl_2O_4 + Ni^0 \rightarrow CO(g) + O_x\text{–}Ni \quad \text{rapid} \tag{4}$$

$$Ni^0\text{–}CH_x + Ni^0 - O_x \rightarrow CO(g) + H_2(g) + 2Ni^0 \quad \text{slow} \tag{5}$$

The continuous formation of CO and H_2 evidenced this assumption.

The exact form and properties of this "oxygen pool" were not clearly elucidated until now although it was proposed the possible form of adsorbed oxygen, hydroxide or carbonate. Ferreira-Aparicio et al. [24] found that the carbonate type species, when CH_4 was introduced to the reactant flow, decreased and is replaced by adsorbed formate species, which were depleted after carbon dioxide is removed from the mixture. Different trends were observed over our catalysts. As illustrated in Figs. 3 and 6, adsorption of CO_2 over the support or catalyst produced large amount of formate species, which can be enhanced by CH_4 introduction (Figs. 5 and 7). This implies that these species can transform from one to another. This requires the participation of mobile oxygen species and hydrogen species. Surface hydroxyl groups (surface hydroxide or HCO_3) on the support may serve as carriers that allow mobility of these species. As for alumina-based support, this can be carried out through surface hydroxyl group over Al:

$$4Al\text{–}OH + 2CO \leftrightarrow 2Al\text{–}O\text{–}COOH + Al\text{–}O\text{–}Al + H_2O \tag{6}$$

$$2Al\text{–}OH + CO \leftrightarrow Al\text{–}O\text{–}CO\text{–}O\text{–}Al + H_2O \tag{7}$$

A few papers have been published in which oxycarbonates were detected in both Ru and Ni catalysts supported on La_2O_3 [8]. These authors concluded that the formation of oxycarbonates during reaction plays a central role in the CO_2 reforming of methane. But this was seldom addressed in the catalyst when using aluminum-based supports. This could be ascribed to the weak adsorption of CO_2 on these compounds. When MgO was introduced into γ-Al_2O_3 surface, the adsorption of CO_2 was enhanced and the specific role of carbonate species was further elucidated in our samples. The temperature-programmed oxidation, temperature-programmed hydrogenation and temperature-programmed CO_2 reaction profiles showed that there were three carbon species (i.e., C_α, C_β and C_γ) on $Ni/MgAl_2O_4$ surface [3]. C_γ was responsible for catalyst deactivation. The C_γ species was found to be the most inactive species toward H_2 and O_2. In contrast, the C_γ species was unexpectedly more active toward CO_2 than C_α and C_β on $Ni/MgAl_2O_4$ surface. The unique reactivity of CO_2 with different coke species could be ascribed to the carbonate, bidentate and formate species formation on $MgAl_2O_4$ surface. These surface species enhanced the oxidation of C_γ and thus contributed to the high stability of $Ni/MgAl_2O_4$ catalyst. In the dry reforming conditions with a high temperature, the surface hydroxyl groups desorbed easily, and CO_2 decomposition was depressed. In the present study, when CO_2 was adsorbed on the support, no CO was formed except carbonate species was observed by FTIR in Fig. 6.

These conclusions may find support in the literature. Bitter et al. [25] have suggested that Pt/ZrO_2 catalysts are not efficient for dry reforming of methane when formation of carbonates is not possible. Recently, Zhang et al. [26] also found that $La_2O_2CO_3$ and formate species may participate in the surface chemistry to produce synthesis gas over a high stable Ni/La_2O_3 catalyst. From the above proposed mechanism, the formation of carbonate and formate type species is also an important intermediate for the reaction of CH_x with CO_2 over Ni catalyst. Although different catalytic performances usually observed considering the Ni and noble metal catalysts (such as lower carbon deposition and hither activity), the Ni-based catalyst can be more active and resistant to coke accumulation when supported on appropriate catalyst support, which allows a more effective CO_2 activation.

5. Conclusions

The catalyst support, $MgAl_2O_4$, plays an essential role in surface carbonaceous species with CO_2, including assisting nickel to form highly and uniformly dispersed metallic nickel particles after reduction through the interaction between the active phase Ni and the support; allowing an effective way for CO_2 activation through formation of carbonate/bicarbonate type species, which contributes to the long-term stability and specific carbon elimination. The activation of methane through dehydrogenation progressively was confirmed by the observation of CH_x species directly on Ni catalyst. The mechanistic aspect of surface active carbonaceous species with CO_2 over $Ni/MgAl_2O_4$ catalysts was recommended according to these results. The surface carbonate species may migrate to the metal–support interfacial region or may spill over onto the metal surface to react with CH_x. This reaction provides a rationale for the stability of this catalyst.

Acknowledgment

Financial support from the Chinese National Natural Science Foundation (Project Nos. 20343002 and 20433030) is gratefully acknowledged.

References

[1] J.H. Lunsford, Catal. Today 63 (2000) 165–174.
[2] C.A. Querini, in: J.J. Spivey, G.W. Roberts (Eds.), Catalysis, vol. 17, The Royal Society of Chemistry, 2004, pp. 166–209.
[3] J.J. Guo, H. Lou, X.M. Zheng, Carbon 45 (2007) 1314–1321.
[4] J.J. Guo, H. Lou, H. Zhao, D.F. Chai, X.M. Zheng, Appl. Catal. A 273 (2004) 75–82.
[5] J.J. Guo, H. Lou, X.M. Zheng, React. Kinet. Catal. Lett. 84 (2005) 93–100.
[6] C.H. Bartholomew, J.B. Butt, Catalysts Deactivation, Elsevier Science Publishers, Amsterdam, 1991.
[7] M.C.J. Bradford, M.A. Vannice, J. Catal. 173 (1998) 157–171.
[8] J.F. Múnera, S. Irusta, L.M. Cornaglia, E.A. Lombardo, D.V. Cesar, M. Schmal, J. Catal. 245 (2007) 25–34.
[9] X.E. Verykios, Int. J. Hydrogen Energy 28 (2003) 1045–1063.
[10] L.Y. Mo, J.H. Fei, C.J. Huang, X.M. Zheng, J. Mol. Catal. A 193 (2003) 177–184.
[11] H.P. Klug, L.E. Alexander, X-ray Diffraction Procedures for Polystalline and Amorphous Materials, 2nd ed., Wiley–Interscience, New York, 1974, 148 pp.
[12] G. Ertl, H. Knozinger, J. Weitkamp, Hangdbook of Heterogeneous Catalysis, Wiley, Weinheim, 1997, 442 pp.
[13] L.M. Aparicio, J. Catal. 165 (1997) 262–274.
[14] T. Osaki, H. Masuda, T. Mori, Catal. Lett. 44 (1997) 19–21.
[15] G. Socrates, Infrared and Raman Characteristic Group Frequencies-tables and Charts, Wiley, New York, 2004, 338 pp.
[16] T. Osaki, J. Chem. Soc., Faraday Trans. 93 (1997) 643–647.
[17] A. Davydov, Molecular Spectroscopy of Oxide Catalyst Surfaces, Wiley, Chester, 2003, 134 pp.
[18] M.M. Schubert, H.A. Gasteiger, R.J. Behm, J. Catal. 172 (1997) 256–258.
[19] G. Heerberg, Molecular Spectra and Molecular Structure. II. Infrared and Raman Spectra of Polyatomic Molecules, Van Nostrand, New York, 1945, 274 pp.
[20] A.M. Efstathiou, A. Kladi, V.A. Tsipouriari, X.E. Verykios, J. Catal. 158 (1996) 64–75.
[21] V.C.H. Kroll, H.M. Swaan, S. Lacombe, C. Mirodatos, J. Catal. 164 (1996) 387–398.
[22] B.Q. Xu, J.M. Wei, Y.T. Yu, J.L. Li, Q.M. Zhu, Top. Catal. 22 (2003) 77–85.
[23] A.N.J. van Keulen, K. Seshen, J.H.B.J. Hoebink, J.R.H. Ross, J. Catal. 166 (1997) 306–314.
[24] P. Ferreira-Aparicio, I. Rodriguez-Ramos, J.A. Anderson, A. Guerrero-Ruiz, Appl. Catal. A 202 (2002) 183–196.
[25] J.H. Bitter, K. Seshan, J.A. Lercher, J. Catal. 171 (1997) 279–286.
[26] Z. Zhang, X.E. Verykios, S.M. MacDonald, S. Affrossman, J. Phys. Chem. 100 (1996) 744–754.